Spectrochimica Acta Part A: Molecular and Biomolecular Spectroscopy 138 (2015) 38–48

Contents lists available at ScienceDirect

Spectrochimica Acta Part A: Molecular and Biomolecular Spectroscopy

journal homepage: www.elsevier.com/locate/saa

Silicon-containing bis-azomethines: Synthesis, structural characterization, evaluation of the photophysical properties and biological activity

Mirela-Fernanada Zaltariov [a], Angelica Vlad [a], Maria Cazacu [a,*], Mihaela Avadanei [a], Nicoleta Vornicu [b], Mihaela Balan [a], Sergiu Shova [a]

[a] "Petru Poni" Institute of Macromolecular Chemistry, Aleea Gr. Ghica Voda 41A, 700487 Iaşi, Romania
[b] Metropolitan Center of Research TABOR, The Metropolitanate of Moldavia and Bukovina, Closca 9, 700066 Iaşi, Romania

HIGHLIGHTS

- An original diamine containing dimethylsilane unit was obtained and characterized.
- Azomethines of salicylaldehyde and its OH- and CH_3O-substituted derivatives were obtained.
- Schiff bases proved to be good UV light absorbing and fluorescent materials.
- The photophysical sensitivity to the solvent polarity was studied.
- Two azomethines proved antimicrobial activity better than standard compounds.

GRAPHICAL ABSTRACT

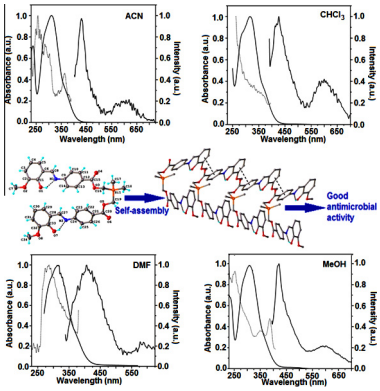

ARTICLE INFO

Article history:
Received 25 July 2014
Received in revised form 23 October 2014
Accepted 5 November 2014
Available online 13 November 2014

Keywords:
Amine
Azomethine
Structural characterization
Photophysical properties
Biological activity

ABSTRACT

A new diamine, (dimethylsilanediyl)bis(methylene)bis(4-aminobenzoate) (**1**), containing dimethylsilane spacer, was prepared by the condensation of p-aminobenzoic acid with bis(chloromethyl)dimethylsilane. This was subsequently reacted with salicylaldehyde, 3-hydroxy-salicylaldehyde, and 3-methoxy-salicylaldehyde, when corresponding Schiff bases (*E*)-(dimethylsilanediyl)bis(methylene)bis(4-((*E*)-(2-hydroxybenzilidene)amino)benzoate (**2**), (*E*)-(dimethylsilanediyl)bis(methylene)bis(4-((*E*)-(2-hydroxybenzilidene)amino)benzoate (**3**), and (*E*)-(dimethylsilanediyl)bis(methylene) bis(4-((*E*)-(2-hydroxy-3-methoxybenzilidene)amino)benzoate (**4**), respectively were formed. All the obtained compounds were structurally characterized by spectral (FT-IR, ^{1}HNMR, ^{13}CNMR) analyses and single crystal X-ray diffraction. Photophysical studies revealed that the new prepared Schiff bases are good UV light absorbing and fluorescent materials. Thus, they exhibit strong UV/Vis-absorption at 250–400 nm and violet or orange emission, in sensitive dependence on the polarity of the solvents and the nature of the substituent (—H, —OH and —OCH_3) at the aromatic ring. The antimicrobial activity of these compounds was first studied *in vitro* by the disk diffusion assay against two species of bacteria and three fungi. The minimum inhibitory concentration was then determined with the reference of standard compounds. The results displayed that Schiff bases **3** and **4** having hydroxy- and methoxy-substituents on the aromatic ring were better inhibitors of both types of species (bacteria and fungi) than standard compounds, Caspofungin and Kanamycin.

* Corresponding author.
E-mail address: mcazacu@icmpp.ro (M. Cazacu).

http://dx.doi.org/10.1016/j.saa.2014.11.007
1386-1425/

Introduction

Schiff bases, also known as azomethines, are some of the most widely used organic compounds in different fields such as medicine (in synthesis of medicinal compounds) [1–3], biology (as biochemical and antimicrobial reagents due to similarities with natural biological compounds) [4], analytical chemistry (reagents or optical, electrochemical, and chromatographic sensors) [5,6], and materials chemistry (catalysts, pigments and dyes, polymer stabilisers, light emitting diodes OLED, PLED) [7,8], as oxygen carriers [9,10], as ligands and intermediates in organic synthesis [7]. Their properties (chemical, optical, magnetic, electrical) can be tuned by the proper choice of the precursors – amine and carbonylic compounds.

Schiff bases of "*salen-type*" based on a diamine and salicylaldehyde derivatives are among the most versatile ligands due to their easy preparation and ability to bind a variety of metal ions [8,11–19]. Like almost all the azomethines, those of *salen-type* as well as their metal complexes have exhibited many potential applications in different areas, such as catalysts [18,20–23], and sensors [24], optical [25–27] and magnetic materials [27,28], biological agents [29], non-linear optics (NLOs) [30], electrochemical sensing [31]. Those containing chromophore groups proved to be important building blocks for luminescent complexes [18,20–35]. Depending on the chosen amine, the *salen-type* metal complexes can conformationally be more rigid or flexible, the last being able to adopt a variety of geometries and to generate various active site environments for the different oxidation reactions. This flexibility, similar to that observed in metalloproteins, is a key factor for the biomimetic activity of these molecules [36]. Our previous works demonstrated that introducing the siloxane groups to *salen-type* ligands could confer hydrophobicity, structural flexibility and self-assembling ability [37,38].

In this paper we prepared a new diamine containing a dimethylsilane unit that was condensed with salicylaldehyde and two of her substituted (—OH and —OCH_3) derivatives. It would be expected that the presence of carbosilane groups with its particularities (higher length and polarization as compared to C—C bond, hydrofobicity) to confer uniqueness in structures in which they are included and their properties. While the presence of salicylaldehyde chromophore could induce light absorption-emission capacity [39], it is expected as the co-existence of azomethine groups to confer biological activity [40]. After structural characterization, the photophysical and antimicrobial properties of the resulted Schiff bases were studied here.

Experimental

Materials and measurements

4-aminobenzoic acid (Aldrich), bis(chloromethyl)dimethylsilane (Fluka), 2-hydroxybenzaldehyde, 2,3-dihydroxybenzaldehyde and 2-hydroxy-3-methoxybenzaldehyde (Aldrich), sodium hydroxide (Aldrich), methanol (Chimopar), chloroform (Chimopar), dimethylformamide (Aldrich), petroleum ether (Chimopar), acetonitrile (Aldrich), acetone (Chimopar) were used as received.

Fourier transform infrared (FT-IR) spectra were recorded using a Bruker Vertex 70 FT-IR spectrometer. Registrations were performed in the transmission mode in the range 400–4000 cm^{-1} at room temperature with a resolution of 2 cm^{-1} and accumulation of 32 scans.

The NMR spectra were recorded on a BrukerAvance DRX 400 MHz Spectrometer equipped with a 5 mm QNP direct detection probe and z-gradients. Spectra were recorded in $CDCl_3$, at room temperature. The chemical shifts are reported as δ values (ppm). The atom labeling for the NMR assignments is that from XRD structures. The assignments of all the signals in the 1D NMR spectra were done using 2D NMR experiments like H,H-COSY, H,C-HMQC and H,C-HMBC.

X-ray crystallography

Crystallographic measurements for compounds **1**-**4** were carried out with an Oxford-Diffraction XCALIBUR E CCD diffractometer equipped with graphite-monochromated Mo Kα radiation. Single crystals were positioned at 40 mm for **1** and **2** (45 mm for **3** and **4**) from the detector and 224, 559, 237, and 272 frames were measured each for 20, 5, 140, and 60 s over 1° scan width for **1**, **2**, **3** and **4**, respectively. The unit cell determination and data integration were carried out using the CrysAlis package of Oxford Diffraction [41]. All the structures were solved by direct methods using Olex2 [42] software with the SHELXS structure solution program and refined by full-matrix least-squares on F^2 with SHELXL-97 [43]. Atomic displacements for non-hydrogen, non-disordered atoms were refined using an anisotropic model. Both asymmetric molecules in the crystal structure **1** were found to be disordered in two orientations with occupancy factors 0.8 and 0.2. The positional parameters of disordered atoms were refined using available tools (PART, DFIX, and SADI) of SHELXL97 and the combined anisotropic/isotropic refinement has been applied for non-hydrogen atoms. The hydrogen atoms have been placed by Fourier Difference accounting for the hybridisation of the supporting atoms and the possible presence of hydrogen bonds in the case of donor atoms. The molecular plots were obtained using the Olex2 program [42].

The absorption and emission measurements were carried out in four solvents of spectral grade: DMF, chloroform, methanol and acetonitrile. UV–Vis absorption spectra of solutions were recorded on a Specord 200 spectrophotometer, in a quartz cell with path length of 1.0 cm. Fluorescence spectra were obtained by using a Perkin Elmer LS55 luminescence spectrometer, in the same cell.

In vitro antimicrobial activity tests against the bacterial species *Pseudomonas aeroginosa*, *Bacillus* sp., and fungal species *Aspergillus flavus, Penicillium chrysogenum*, *Alternaria alternate*, were performed according to standard procedures (SR-EN 1275:2006 and NCCLS:1993) on agar-type media, by the disc diffusion method.

Syntheses

Synthesis of (dimethylsilanediyl)bis(methylene)bis(4-aminobenzoate), 1

A mixture of 4-aminobenzoic acid sodium salt (3.18 g, 20 mmol) and bis(chloromethyl)dimethylsilane (1.46 mL, 10 mmol) in 20 mL DMF was heated to reflux for 8 h (Scheme 1Sa). After separation of NaCl by filtration, the resulted filtrate was precipitated in water, resulting a beige solid. The solid was then dissolved in chloroform and washed with water (3 × 100 mL). The organic extracts were dried over Na_2SO_4, filtrated and concentrated under reduced pressure to afford the desired pure product. Colorless crystals were obtained by recrystallization from chloroform (2.84 g, 79%; m.p. 119 °C).

IR ν_{max} (KBr), cm^{-1}: 3442m, 3398m, 3347s, 3233m, 2958vw, 2930w, 2917w, 2893w, 1693vs, 1648s, 1599vs, 1573m, 1515s, 1441w, 1431w, 1416m, 1316vs, 1305s, 1296vs, 1264s, 1246s, 1172vs, 1117s, 1079m, 1012vw, 962vw, 948vw, 883w, 868m, 855m, 842m, 819w, 792w, 770s, 746w, 698m, 681w, 638w, 623w, 613w, 599m, 510w, 498w, 410vw.

^{1}H-NMR ($CDCl_3$, 400.13 MHz, δ, ppm): 7.86 (d, 4H, H6, 10, 14, 18), 6.60 (d, 4H, H7, 9, 15, 17), 4.13 (s, 8H, —NH_2, H3, 11), 0.29 (S, 6H, H1, 2).

^{13}C-NMR ($CDCl_3$, 100.16 MHz, δ, ppm): 167.34 (C4, 12), 150.69 (C8, 16), 131.55 (C6, 10, 14, 18), 119.89 (C5, 13), 113.80 (C7, 9, 15, 17), 55.34 (C3, 11), −5.70 (C1, 2).

Synthesis of the Schiff base compounds

Synthesis of (E)-(dimethylsilanediyl)bis(methylene)bis(4-((E)-(2-hydroxybenzilidene)amino)benzoate, 2. A mixture of **1** (0.50 g, 1.4 mmol) and 2-hydroxybenzaldehyde freshly distilled (0.34 g, 2.8 mmol) in methanol/chloroform solvents mixture (2:1 v/v) was stirred to reflux for 4 h. A yellow precipitate was formed, that was filtered, washed with petroleum ether and then crystallized from acetonitrile (0.65 g, 82%; m.p. 126 °C).

IR ν_{max} (KBr), cm^{-1}: 3420w, 3055vw, 2959w, 2922vw, 2897w, 1720vs, 1620s, 1599vs, 1570s, 1491m, 1454m, 1418m, 1364m, 1310vs, 1256s, 1231s, 1171vs, 1113s, 1032w, 1011w, 972w, 951vw, 935vw, 908w, 881m, 862s, 833m, 795m, 770s, 752s, 689m, 611vw, 555vw, 517w, 447w, 403w.

^{1}H-NMR ($CDCl_3$, 400.13 MHz, δ, ppm): 12.94 (s, 2H, —OH), 8.64 (s, 2H, H7, 26), 8.08 (d, 4H, H10, 12, 21, 25), 7.46–7.42 (m, 4H, H3, 5, 29, 30), 7.30 (d, 4H, H9, 13, 22, 24), 7.06 (d, 2H, H2, 31), 6.69 (t, 2H, H4, 29), 4.25 (s, 4H, H15, 18), 0.36 (s, 6H, H16, 17).

^{13}C-NMR ($CDCl_3$, 100.16 MHz, δ, ppm): 166.67 (C14, 19), 164.10 (C7, 26), 161.22 (C1, 32), 152.40 (C8, 23), 133.80 (C3, 30), 132.65 (C5, 28), 130.97 (C10, 12, 21, 25), 128.38 (C11, 20), 121.11 (C9, 13, 22, 24), 119.27 (C4, 29), 118.92 (C6, 27), 117.35 (C2, 31), 56.24 (C18, 18), −5.65 (C16, 17).

Synthesis of (E)-(dimethylsilanediyl)bis(methylene)bis(4-((E)-(2,3-dihydroxybenzilidene)amino)benzoate, 3. A mixture of **1** (0.50 g, 1.4 mmol) and 2,3-dihydroxybenzaldehyde (0.39 g, 2.8 mmol) in methanol/chloroform solvents mixture (2:1 v/v) was stirred at room temperature for 24 h. A red precipitate appeared after 20 h that was filtered, washed with petroleum ether and dried. Crystals from **3** were obtained by recrystallization from chloroform/acetonitrile solvents mixture (0.72 g, 86%; m.p. 146 °C).

IR ν_{max} (KBr), cm^{-1}: 3479m, 3061vw, 2959w, 2914w, 1719vs, 1622m, 1601m, 1580s, 1504w, 1460s, 1420m, 1364m, 1312s, 1273s, 1256s, 1213s, 1173s, 1115s, 1074w, 1032w, 1011w, 972vw, 939vw, 851s, 787m, 766m, 731s, 692w, 608w, 557w, 492w, 455vw, 407w.

^{1}H-NMR ($CDCl_3$, 400.13 MHz, δ, ppm): 13.41 (s, 2H, OH1, 32), 8.63 (s, 2H, H7, 26), 8.06 (d, 4H, H10, 12, 21, 25), 7.28 (d, 4H, H9, 13, 22, 24), 7.11 (d, 2H, H3, 30), 6.99 (d, 2H, H5, 28), 66.88 (t, 2H, H4, 29), 5.90 (s, 2H, OH2, 31), 4.26 (s, 4H, H15, 18), 0.36 (s, 6H, H16, 17).

^{13}C-NMR ($CDCl_3$, 100.16 MHz, δ, ppm): 166.59 (C14, 19), 163.72 (C7, 26), 151.60 (C8, 23), 149.23 (C1, 32), 145.12 (C2, 31), 131.04 (C10, 12, 21, 25), 128.57 (C11, 20), 123.32 (C5, 28), 120.98 (C9, 13, 22, 24), 119.37 (C4, 29), 118.39 (C3, 30), 118.34 (C6, 27), 56.40 (C15, 18), −5.70 (C16, 17).

Synthesis of (E)-(dimethylsilanediyl)bis(methylene) bis(4-((E)-(2-hydroxy-3-methoxybenzilidene)amino)benzoate, 4. A mixture of **1** (0.50 g, 1.4 mmol) and 2-hydroxy-3-methoxybenzaldehyde (0.43 g, 2.8 mmol) in methanol/chloroform solvents mixture (2:1 v/v) was stirred at room temperature for 2 h and then to reflux for 8 h. After the evaporation of the solvents mixture, the resulting orange product was crystallized from acetone. Orange crystals appeared after three weeks at 4 °C (0.78 g, 90%; m.p. 158 °C).

IR ν_{max} (KBr), cm^{-1}: 3441w, 2997vw, 2941w, 2918vw, 2841vw, 1719s, 1699s, 1616s, 1595s, 1572s, 1503w, 1464vs, 1441m, 1412m, 1369w, 1319s, 1308s, 1258vs, 1198s, 1173s, 1115m, 1101s, 1078m, 1015w, 972m, 866m, 854m, 833m, 812m, 785m, 773m, 741s, 700m, 660vw, 584w, 567w, 505vw, 415vw, 392vw.

^{1}H-NMR ($CDCl_3$, 400.13 MHz, δ, ppm): 13.31 (s, 2H, OH), 8.66 (s, 2H, H8, 27), 8.10 (d, 4H, H11, 13, 22, 26), 7.31 (d, 4H, H10, 14, 23, 25, overlap with solvent rezidual peak), 7.04–7.07 (m, 4H, H3, 5, 29, 31), 6.92 (t, 2H, H4, 30), 4.25 (s, 4H, H16, 19), 3.98 (s, 6H, H7, 34), 0.36 (s, 6H, H17, 18).

^{13}C-NMR ($CDCl_3$, 100.16 MHz, δ, ppm): 166.67 (C15, 20), 164.11 (C8, 27), 152.12 (C9, 24), 151.52 (C1, 33), 148.49 (C2, 32), 131.00 (C11, 13, 22, 26), 128.47 (C12, 21), 124.09 (C5, 29), 121.14 (C10, 14, 23, 25), 118.88 (C6, 28), 118.79 (C4, 30), 115.34 (C3, 31), 56.23 (C7, 16, 19, 34), −5.63 (C17, 18).

Results and discussion

A new diamine, containing dimethylsilane group as a spacer, (dimethylsilanediyl)bis(methylene)bis(4-aminobenzoate), **1**, was prepared by the condensation of 4-aminobenzoic acid with a bis(chloromethyl)dimethylsilane (Scheme 1Sa). The reaction occurred in DMF at reflux, for 8 h.

FTIR and NMR spectroscopy

In the FTIR spectrum of the new silicon-containing diamine, there are present the absorption bands characteristic for primary aromatic amine at 3442, 3347, and 3233 cm^{-1}, while those for ester group appear at 1693 cm^{-1}, and for dimethylsilane moiety at 842 and 1246 cm^{-1} (Fig. 1S).

In the ^{1}H NMR spectrum of the diamine, the signals of aromatic protons appear at 7.86 and 6.40 ppm, while the peak corresponding to resonance of the amine protons appear at 4.13 ppm (Fig. 2S). Other peaks are those at 0.29 and 4.13 ppm corresponding to the protons from Si—CH_3 and Si—CH_2, respectively. Their intensities ratio (Ar: —NH_2: Si—CH_3: Si—CH_2 = 2:1:1.5:1) corresponds to the presumed structure. The 2D NMR experiments used for the characterization of compound **1** are shown in Figs. 3S and 4S. ^{13}C NMR spectrum also confirms the formation of the diamine **1** (Fig. 5S).

The diamine **1** was reacted with salicylaldehyde, 3-hydroxy-salicylaldehyde, and 3-methoxy-salicyladehyde in 1:2 molar ratio under similar conditions resulting corresponding Schiff bases: (*E*)-(dimethylsilanediyl)bis(methylene)bis(4-((*E*)-(2-hydroxybenzilidene)amino)benzoate (**2**), (*E*)-(dimethylsilanediyl)bis(methylene)bis(4-((*E*)-(2-hydroxybenzilidene)amino)benzoate (**3**), and (*E*)-(dimethylsilanediyl)bis(methylene) bis(4-((*E*)-(2-hydroxy-3-methoxybenzilidene)amino)benzoate (**4**), respectively, according to Scheme 1Sb. The formation of these condensation products was easily confirmed by their IR and ^{1}H-NMR spectra. Thus, FT-IR spectra of the resulted azomethines show characteristic absorption bands attributed to the azomethine group (—CH = N—) at 1620 cm^{-1} (**2**), 1622 cm^{-1} (**3**), and 1616 cm^{-1} (**4**), Si—CH_3 at 833–851 cm^{-1} and 1256–1258 cm^{-1}, and ($\nu_{C=O}$) from ester groups at 1719–1720 cm^{-1} (Fig. 6S).

The ^{1}H-NMR spectra of all Schiff bases prove the formation of the imine bond by the presence of the peak corresponding to —C*H*=N— proton at 8.66 ppm (**4**), 8.64 ppm (**2**), 8.63 ppm (**3**) and the specific aromatic protons from the diamine and aldehyde units with some modifications compared with the starting compounds. The peaks corresponding to proton resonance from dimethylsilane unit appear at 0.35–0.36 ppm and that assigned to —CH_2— at 4.25–4.26 ppm, their intensity ratio corresponding to the presumed structures (Figs. 7S, 12S, 17S).

The positions of the peaks in ^{13}C NMR spectra are also in concordance with the structures depicted in Scheme 1Sb (Figs. 11S, 16S, 21S).

The 2D NMR experiments used for the characterization of the resulted Schiff base compounds are shown in Figs. 8S–10S, 13S–15S and 18S–21S for the compounds **2**, **3** and **4**, respectively.

The obtained imines were of high purity, as single crystals, and are stable at room temperature in the solid state.

Crystal structure of Schiff base compounds

According to X-ray crystallography all studied compounds (**1**-**4**) have a similar molecular crystal structure comprising the corresponding neutral entities without any co-crystallized solvent molecules. The results of X-ray diffraction studies of the compounds **1**–**4** together with atomic numbering schemes are shown in Figs. 1–4. The crystallographic data and refinement details are quoted in Table 1, while selected geometrical parameters in Tables 1S–4S.

CCDC-980507 (**1**), CCDC-980508 (**2**), CCDC-980506 (**3**), CCDC-980509 (**4**), contain the supplementary crystallographic data for this contribution. These data can be obtained free of charge via www.ccdc.cam.ac.uk/conts/retrieving.html (or from the Cambridge Crystallographic Data Centre, 12 Union Road, CambridgeCB2 1EZ, UK; fax: (+44) 1223-336-033; or deposit@ccdc.ca.ac.uk).

The crystal structure of compound **1** contains two molecules in the unit cell as crystallographically independent units. Both asymmetric units (denoted **A** and **B**) in **1** as well as the molecules **2**-**4** are in the same *cis-oide* conformation and exhibit similar geometric parameters (Table 1S). It should be mentioned, that in the case of **1** and **2** the *cis-oide* conformation is supported by the intramolecular sandwich-type stacking interactions with centroid-to-centroid distances of 4.064 Å for **A**, 3.859 Å for **B** in structure **1** and 3.601 Å, 3.642 Å for two pairs of aromatic rings in structure **2**. No intramolecular π–π interactions have been found in the crystals **3** and **4**. In the structure **1**, these interactions are also associated with the intermolecular N—H···N hydrogen bonding, as it is shown in Fig. 1. Hydrogen-bond parameters for structures **1**–**4** are quoted in Table 2. The crystal structure packing of the compounds **1**–**4** differs, depending on the conditions for intermolecular stacking interactions and the presence of the groups suitable for the role of potential proton donors or proton acceptors. The analysis of the data presented in Table 2 indicate, that there exist various conditions for the intermolecular hydrogen bonding in the crystal structure **1** and **3**. By contrary, in the compounds **2** and **4** all the proton donor groups are involved in the formation of intramolecular hydrogen bonds. On the other hand, the intermolecular sandwich-type stacking interactions are present only in the crystal structure of **3** and **4**, where the centroid-to-centroid distances are of 3.953, 4.185 and 3.829 Å, respectively. Thus, the crystal structure of **2** is built up from the parallel packing of the isolated molecules with the formation of 2D layers, as shown in Fig. 22S. The main crystal structure motif in **1** can be characterized as a band-like supramolecular architecture associated via intermolecular H-bonds and intramolecular π–π stacking (Fig. 23S). The neutral molecules **4** are linked in the crystal space through the intermolecular π–π stacking to form a stepped polymeric chain, the fragment of which is shown in Fig. 24S. The crystal structure **3** represents a tree-dimensional supramolecular network sustained via hydrogen bonding and intermolecular stacking interactions. The view of 3D architecture in **3** is shown in Fig. 25S.

Evaluation of photophysical properties of the diamine and the derived Schiff bases

The absorption profile of diamine **1** is mainly given by an intense band at 282 nm ($\varepsilon > 9.3 \times 10^4$ (L mol^{-1} cm^{-1}) arisen from a benzene transition of the $S_2 \leftarrow S_0(\pi^*, \pi)$ type (Fig. 5). The shoulder around 300 nm could be assigned to a $S_1 \leftarrow S_0(\pi^*, n)$ transition involving the benzene amine moiety. A second band with much lower intensity and centered on 340 nm corresponds to a $\pi \rightarrow \pi^*$ state involving the whole molecule. The emission spectrum recorded at $\lambda_{exc} = 340$ nm presents one and intense band at 436 nm, while the excitation spectrum reveals two resolved contributions that almost match the two bands of the absorption spectrum.

The ground state absorption and fluorescence spectra of compounds **2**–**4** in various solvents are shown in Figs. 6–8. The shape of the spectra is in close relation with the polarity and proton donation capability of the solvent. The absorption, emission and excitation spectral data are gathered in Table 3.

The electronic absorption spectrum of **2** resembles those of other anils, the two main bands being assigned to the intramolecular hydrogen bonded enol tautomer. The first band, around 285 nm, originates from the $S_2 \leftarrow S_0$ (π^*, π) transition in benzene ring [44] and is stable regardless the solvent nature and solute concentration. The broad absorption band with the maximum at 345 nm is given by the $S_1 \leftarrow S_0$ (π^*, π) transition of the enol (OH)

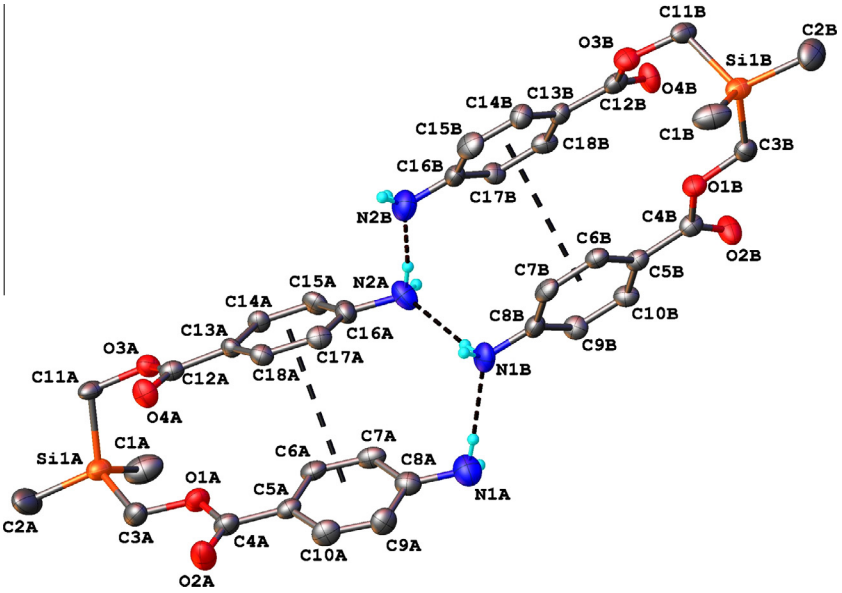

Fig. 1. ORTEP representation of two asymmetric units in the crystal structure of **1**. The thermal ellipsoids are shown at 50% probability level.

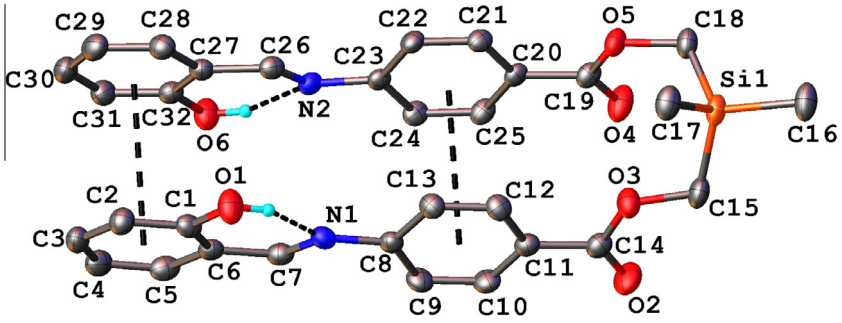

Fig. 2. X-ray molecular structure of compound **2** with thermal ellipsoids drawn at 50% probability level.

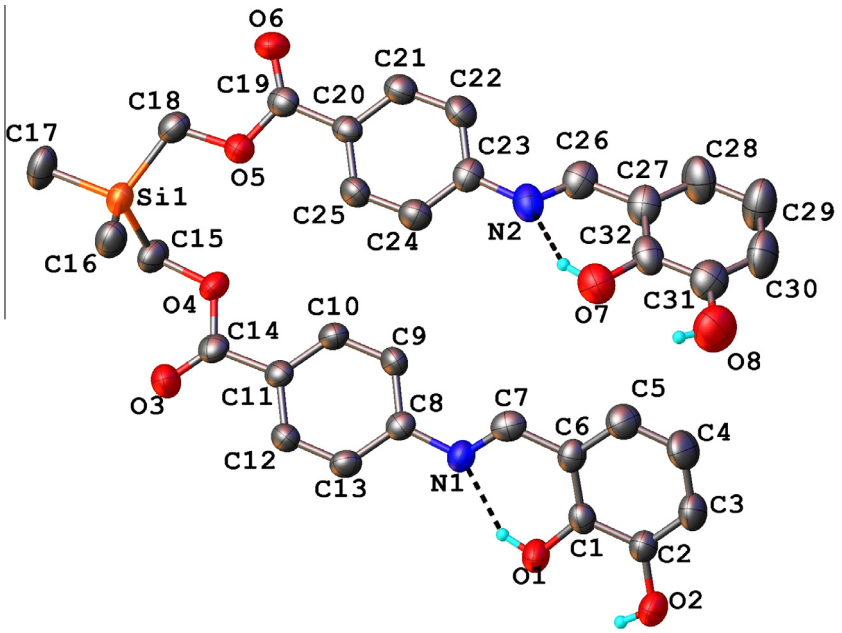

Fig. 3. X-ray molecular structure of compound **3** with thermal ellipsoids drawn at 50% probability level.

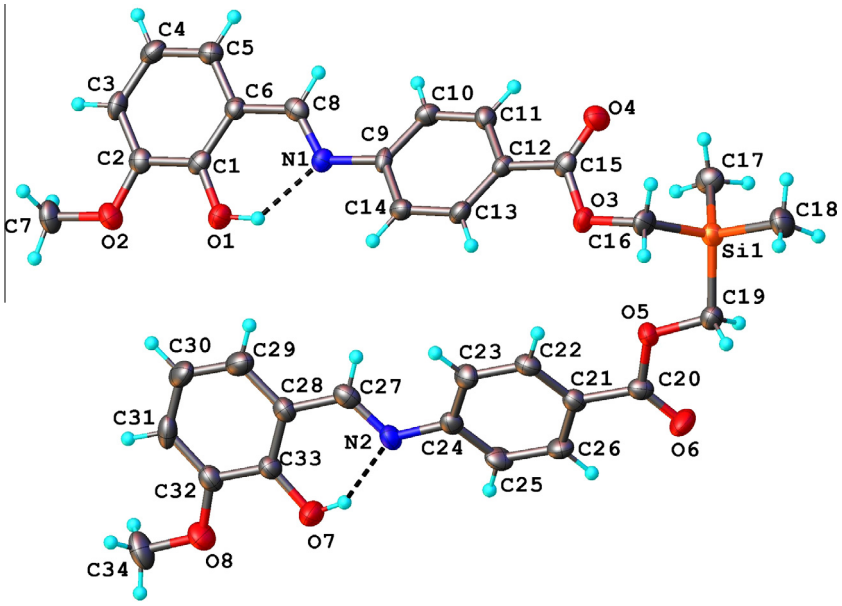

Fig. 4. X-ray molecular structure of compound **4** with thermal ellipsoids drawn at 40% probability level.

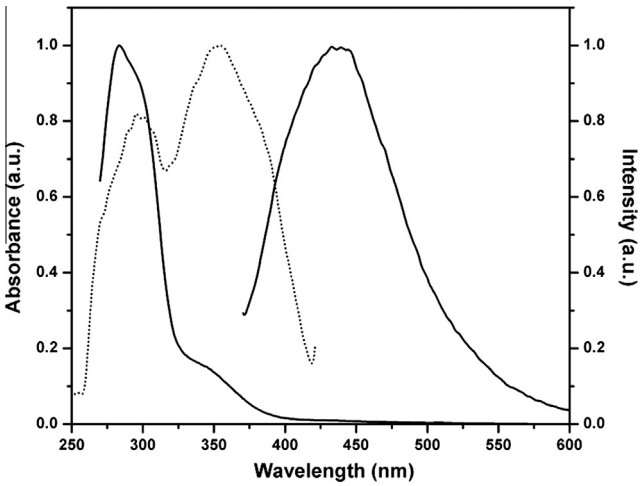

Fig. 5. The absorption, emission (solid traces) and excitation (dotted trace) spectra of **1**.

form and shows a slightly hypsochromic shift with increasing the relative permittivity of the solvent. For the spectrum in MeOH (Fig. 6d), a weak absorption band is observed on the long-wavelength tail, being of very low intensity as compared to that usually observed in the alcoholic solutions of Schiff bases. This band have the maximum around 450 nm, commonly assigned to the $S_1 \leftarrow S_0$ (π^*, π) transition of the proton – transferred keto tautomer in ground state [45,46], to the zwitterionic [47] or to the intermolecular hydrogen bonded complexes with the solvent.

Upon excitation with 345 nm, the emission profile of **2** in the four solvents consists of two weak bands, the first one being the most intense and with the maximum at 415 nm in $CHCl_3$ (Fig. 6b) and DMF (Fig. 6c) and 428 nm in ACN and MeOH solutions (Fig. 6a and d). A second maximum is evident around 530 nm in DMF and $CHCl_3$ solutions, while in ACN and MeOH it is manifesting as a tail beyond 500 nm. The sharp peak at 415–430 nm is usually associated with the emission of excited enol form and shows a mirror image symmetry with the absorption band at 345 nm, from where one can conclude the identity between the absorbing and fluorescent species. The broad and weaker fluorescence band on the long wavelength side shows a large Stoke shift with respect to the absorption band of more than 10,000 cm^{-1}, the magnitude in each solvent being directly correlated with the media polarity. Fig. 6 also shows the excitation spectra of **2** in the four solvents, probed at the emission maxima. Their shape was essentially the same at the two observation wavelengths (420 and 530 nm) and reproduces reasonably the contour of the absorption spectrum, excepting the DMF case (Fig. 6c).

By substitution at the salicylidene ring with groups possessing electron donor and hydrogen bonding abilities it was expected some changes in the absorption spectra to occur, as a result of changes in the electron density of the azomethine group. The absorption spectra of **3** and **4** are very different from that of **2**, but share similar features, showing a single and broad band centered on 319 nm in **3** and 314 nm in **4** (Figs. 7 and 8). The central maximum is given by a $S_1 \leftarrow S_0$ (π^*, π) transition in the salicylidene unit and its extinction coefficient is larger than in **2**, due to increased electron density on the aromatic ring. Also, the redshift extent is larger for **3**, which possess two hydroxyl groups that can be engaged in two different kind of intramolecular hydrogen bonds, so that the imine character of the azomethine bridge is preserved. In contrast, the compound **4** bears only one hydroxyl and its character is quite close to that of the parent compound **2**.

In Figs. 7 and 8 are also presented the fluorescence spectra of **3** and **4** in each of the four solvents. For both compounds, the fluorescence intensity increased with the solvent polarity, so that in $CHCl_3$ the emission is extremely weak. Excitation of **4** in all the solvents within the maximum of the absorption band (i.e. λ_{exc} = 316 nm) shows a distinct peak (around 415 nm) and the raising of a second one at longer wavelength, respectively. The only emission band of

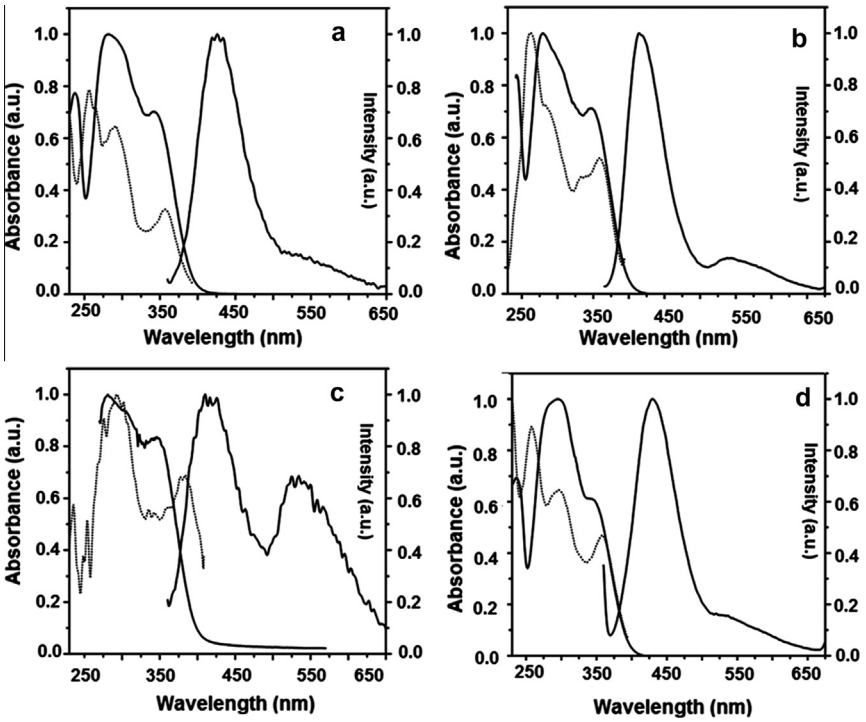

Fig. 6. The absorption, emission (solid traces) and excitation (dotted trace) spectra of **2** in a – ACN, b – $CHCl_3$, c – DMF and d – MeOH.

Table 1
Crystal data and details of data collection for **1–4**.

Compound	1	2	3	4
Empirical formula	$C_{18}H_{22}N_2O_4Si$	$C_{32}H_{30}N_2O_6Si$	$C_{32}H_{30}N_2O_8Si$	$C_{34}H_{34}N_2O_8Si$
Fw	358.47	566.67	598.67	626.72
Space group	$P2_1/n$	$P-1$	$P2_1/c$	$P2_1/n$
a (Å)	16.8345(9)	8.6537(4)	17.818(3)	6.4832(7)
b (Å)	8.7530(8)	10.2342(7)	14.919(2)	17.4066(16)
c (Å)	26.5454(16)	16.3965(11)	11.574(2)	27.748(3)
α (°)	90.00	87.615(5)	90.00	90.00
β (°)	103.456(6)	88.577(5)	104.185(12)	93.423(10)
γ (°)	90.00	76.542(5)	90.00	90.00
V (Å^3)	3804.1(5)	1410.87(15)	2982.9(8)	3125.8(6)
Z	8	2	4	4
λ (Å)	0.71073	0.71073	0.71073	0.71073
ρ_{calcd} (g cm^{-3})	1.252	1.334	1.333	1.332
Crystal size (mm)	0.42 × 0.15 × 0.12	0.55 × 0.20 × 0.10	0.05 × 0.10 × 0.15	0.80 × 0.05 × 0.05
T (K)	200	200	293	173
μ (mm^{-1})	0.147	0.132	0.134	0.131
R_1[a]	0.0869	0.0465	0.0715	0.0661
wR_2[b]	0.1842	0.1121	0.1555	0.0894
GOF[c]	1.066	1.013	0.944	0.942

[a] $R_1 = ||F_o| - |F_c||/|F_o|$.
[b] $wR_2 = \{[w(F_o^2 - F_c^2)^2]/[w(F_o^2)^2]\}^{1/2}$.
[c] GOF = $\{[w(F_o^2 - F_c^2)^2]/(n-p)\}^{1/2}$, where n is the number of reflections and p is the total number of parameters refined.

Table 2
Hydrogen bonding parameters for structures **1–4**.

D—H···A	Distance, Å			Angle D—H···A, °	Symmetry code
	D—H	H···A	D···A		
Compound 1					
N1A—H···O2A	0.86	2.14	2.883(8)	143.7	$x, y-1, z$
N1A—H···N1B	0.86	2.45	3.305(7)	172.9	x, y, z
N1B—H···O2B	0.86	2.12	2.929(9)	155.6	$x, y+1, z$
N1B—H···N2A	0.86	2.34	3.179(6)	166.7	x, y, z
N2A—H···O4A	0.86	2.11	2.905(6)	152.6	$x, y-1, z$
N2A—H···N2B	0.86	2.23	3.079(7)	166.9	x, y, z
N2B—H···O4B	0.86	2.16	2.952(7)	152.3	$x, y+1, z$
Compound 2					
O1—H···N1	0.82	1.86	2.558(2)	147.1	x, y, z
O6—H···N2	0.82	1.89	2.617(2)	147.1	x, y, z
Compound 3					
O1—H···N1	0.82	1.87	2.593(3)	145.7	x, y, z
O7—H···N2	0.82	1.90	2.608(4)	144.7	x, y, z
O2—H···O3	0.82	2.18	2.863(4)	140(4)	$-x, -y, -z-1$
O2—H···O1	0.82	2.23	2.679(3)	114.5	x, y, z
Compound 4					
O1—H···N1	0.84	1.92	2.594(3)	136.2	x, y, z
O6—H···N2	0.82	1.86	2.592(3)	147.2	x, y, z

Table 3
Spectral characteristics of the Schiff bases **2–4.**

Solvent	2				3				4			
	λ_{abs}	$\varepsilon \times 10^3$ (L mol^{-1} cm^{-1})	λ_{em}		λ_{abs}	$\varepsilon \times 10^3$ (L mol^{-1} cm^{-1})	λ_{em}		λ_{abs}	$\varepsilon \times 10^3$ (L mol^{-1} cm^{-1})	λ_{em}	
			λ_{exc} = 345	λ_{exc} = 410			λ_{exc} = 316, 320[a]	λ_{exc} = 380			λ_{exc} = 316, 320[a]	λ_{exc} = 380
MeOH	295	34.6	428	453	315	–	353	418	308	–	352	420
	343	23.8	528 (sh)	534								595
$CHCl_3$	279	65.9	414	450 (w)	318	55.1	420	426	316	38.8	422	422
	347	49.1	537	538				608			594	600
ACN	281	25.8	425	454	315	54.3	412	418	312	46.9	345	430
	343	18.06	535 (sh)	500 (sh)							408	600 (br)
DMF	281	53.3	415	456	318	64.7	382	455	314	73.1	406[b]	453
	346	46.8	428	512								580 (br)

λ_{abs} = maximum of absorption; λ_{em} = maximum of emission; λ_{exc} = excitation wavelength.
[a] Based on the maximum of absorption spectrum.
[b] Varies depending on the concentration sh = shoulder; w = weak; br = broad.

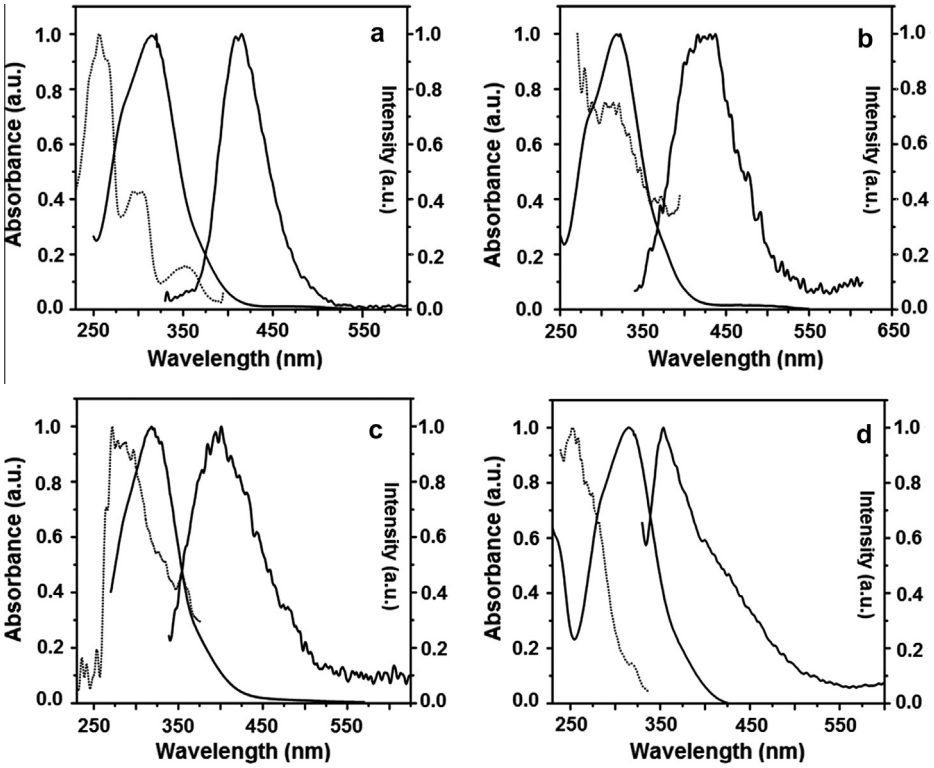

Fig. 7. The absorption, emission (solid traces) and excitation (dotted trace) spectra of **3** in a – ACN, b – $CHCl_3$, c – DMF and d – MeOH.

3 have large variation in position, shifting from 423 nm in $CHCl_3$ to 352 nm in MeOH. The emission maximum of **3** and **4** is located at the highest wavelength for the less polar solvent and presents a hypsochromic shift with increasing the proton donor abilities (MeOH) or the viscosity (DMF) of the solvent.

The excitation spectra recorded at the emission maximum show no resemblance with the absorption in the case of MeOH and $CHCl_3$ solution, but do roughly match it for the ACN and DMF solutions. This would imply that the conformations in the ground and the first excited singlet state in MeOH and $CHCl_3$ are different and there are different emitting species.

The dominant emission at 410–420 nm in all the solvents and at the two excitation wavelengths probed is undoubtedly assigned to the radiative deactivation of the excited phenol–imine structure in the first singlet state. The conformation is the closed form with the intramolecular hydrogen bond untouched. The second emission peak is especially visible under excitation at 380 nm and is centered on 600 nm, therefore it is Stokes-shifted with almost 10,000 cm^{-1}. Due to the high flexibility of the structure given by the long spacer between the two chromophoric units, the second emission probably originates from another *cis*-quinoid conformer with a different geometry.

Summing up all these findings, it can be stated that the substitution in the third position decreased drastically the fluorescence of both excited enol tautomer and that of their proton transferred species, altogether with a significant displacement of the emission wavelengths. Substitution with the hydroxy group almost quenched the proton transfer in salicylidene imine unit. Substitution with the methoxy group led to a different geometry of the keto tautomer, as observed from the fluorescence spectra.

The emission wavelengths for the enol and keto species shifted from blue and emerald green in **2** to purple, violet and amber orange, respectively, in **3** and **4**. One can recognize two enolic species for **3** in ACN and MeOH solutions, which emit purple light, and an enol and a keto form in $CHCl_3$ and DMF, the latter emitting the amber orange light. In DMF, $CHCl_3$ and in a much lesser extent in ACN solution, the absorption band in the 400–500 nm region shows the existence of some species that could be arising from a small amount of *cis*-quinoid tautomer in ground state or intermolecular complexes with the solvent (in the case of $CHCl_3$ and DMF) or might be of zwitterionic nature (in ACN or DMF, due to their high dielectric constant). These structures might be correlated with the weak emission assigned to the radiative deactivation of the excited keto tautomer observed around 600 nm.

The **4**'s fluorescence is originating from at least three species: in MeOH, DMF and $CHCl_3$ solutions we can distinguish two enol forms, which show emission in the purple and violet region, and one keto form, with amber orange fluorescence. In ACN there are two emitting species: one enol (purple light) and one keto, also with amber orange emission. The ESIPT process is responsible for the emission of the keto form in all the four solvents. Direct excitation of the *cis*-quinoid species occurs especially in DMF and MeOH solutions and contributes to the overall fluorescence centered on 600 nm.

Antimicrobial activity studies of the diamine and Schiff bases

For study the antimicrobial activity of the new synthesized compounds (**1**, **2**, **3**, **4**) were chosen three fungi (*Aspergillus flavus* ATCC20046, *Penicillium chrysogenum* ATCC 20044, *Alternaria alternate* ATCC8741) from pure culture and two bacteria (*Pseudomonas aeroginosa* ATCC 27813 and *Bacillus sp.* ATCC 31073) species. The microorganisms were provided by American Type Culture Collection (ATCC), USA. For these determinations we used Petri dishes with culture medium agar – Sabouraud and agar – agar from Merck. The successive dilution procedure has been used to prepare the suspension of microorganisms. Final load of as prepared stock inoculum was $1x10^{-4}$μg/ml.

Culture *in vitro* was performed by the MIC test strip method according to standard procedures (SR-EN 1275:2006 and

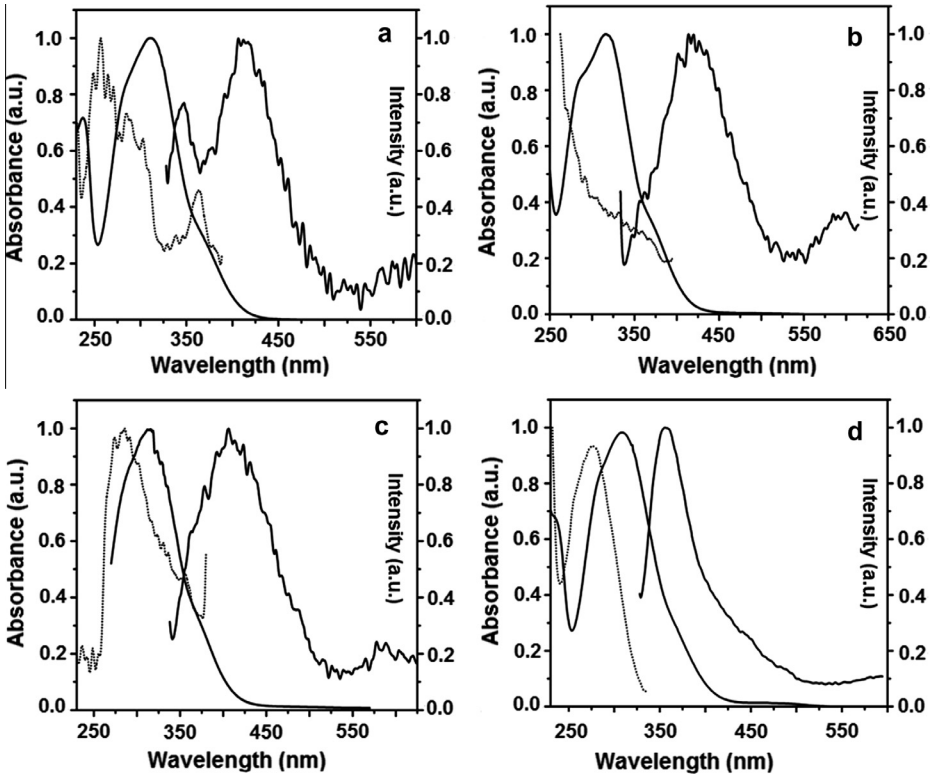

Fig. 8. The absorption, emission (solid traces) and excitation (dotted trace) spectra of **4** in a – ACN, b – $CHCl_3$, c – DMF and d – MeOH.

NCCLS:1993). Caspofugin (small test) was used as a standard for antifungal activity and Kanamycin (small test) was used for antibacterial activity. Standard compounds derived from company Liofilchem.

Culture was performed by using mixture 1:1 microorganism suspension and solution of the compound to be tested that were deposed on the solid medium. The discs were placed on the previously seeded plates and incubated at 37 °C. A blank sample was also prepared in order to verify the influence of the solvent on the biological activity. After 24 h of incubation a symmetrical inhibition ellipse centered along the strip was observed. The MIC is read directly from the scale in terms of μg/mL at the point where the edge of the inhibition ellipse intersects the strip MIC Test Strip. The results of the antibacterial and antifungal activities, MIC values for the tested compounds are given in the Table 4. The biological activity of the Schiff bases is assigned to the formation of the hydrogen bonds through the azomethine group and the active center of the cell constituents. Thus, the biological activity can be explained based on the structure of the compounds, the presence of N, O-donor atoms that polarize the azomethine groups increasing its ability for hydrogen bonds. In Table 4 it can be seen a very good antimicrobial activity in the case of compounds **3** and **4**, due to the co-existence of the azomethine group with —OH (**3**) and —O—CH_3 (**4**) – groups in adequate positions. These two compounds have close values with the reference compounds, Caspofungin and Kanamycin.

Conclusions

Three new azomethines have been obtained based on an original diamine. According to X-ray crystallography, both amine and derived azomethines have a similar molecular crystal structure comprising the corresponding neutral entities without any co-crystallized solvent molecules. UV–Vis and fluorescence studies have revealed a strong dependence of the spectral pattern and bands intensities on the solvents polarity and their proton

Table 4
Antimicrobial tests results.

Sample	MIC (μg/mL)				
	Fungi			Bacteria	
	Aspergillus flavus ATCC20046	Penicillium chrysogenum ATCC 20044	Alternaria alternate ATCC8741	Bacillus sp. ATCC 31073	Pseudomonas aeroginosa ATCC 27813
	Sample concentration, wt%				
	2	2	2	2	2
1	>32	>32	>32	>256	>256
2	>32	>32	>32	>256	>256
3	0.047	0.047	0.032	1.5	1.5
4	0.032	0.032	0.032	1.0	1.0
Caspofungin[a]	0.25	0.25	0.25	–	–
Kanamycin[a]	–	–	–	3	3

[a] Standard compound.

donation capability as well as effect of the substituent at the aromatic ring. Thus, the effect of substitution on the photophysical properties of the diimines in ground and excited states was investigated in four solvents, differentiated by their dielectric permittivity and by ability to form hydrogen bonds with the compounds molecules. Results evidenced several different conformers and tautomers, which have been connected with the chemical structure of the substitution group and with the solvent nature. As the parent compound showed emission from both excited primary enol and hydrogen atom transferred form, the fluorescence of the substituted imines was almost quenched. The reduction of the proton/hydrogen atom transfer was very efficient in compound **3**, where the presence of the second alcohol group shifted the enol – keto/quinoid equilibrium towards the primary enol structure. Most probably, the stabilization of the phenol – imine structure of **3** is achieved through the additional inter- and intramolecular hydrogen bonds. The color emission of the substituted diimines had shifted accordingly, from blue and emerald green in **2** to purple, violet and amber orange, respectively, in **3** and **4**. The fluorescence spectra also revealed that, the hydrophobic nature of the bridge between the azomethine chromophores in the three Schiff bases, leads to the aggregation at a micrometer scale in different solvents. The results of the antimicrobial activity tests revealed increased efficiency, close to that of the reference compounds Caspofungin and Kanamycin, in the case of the azomethines derived from substituted salicylaldehyde.

Acknowledgments

This research was founded by the Romanian Ministry of National Education under Grant 53/02.09.2013, Cod: PN-II-ID-PCE-2012-4-0261.

Appendix A. Supplementary material

Reaction scheme, FTIR, ^{1}H NMR, H,C-HMQC, H,C-HMBC, ^{13}C-RMN spectra for compounds **1-4**, H,H-COSY spectra for the compounds **2-4**, and packings for compounds **1-4** are provided. Supplementary data associated with this article can be found, in the online version, at http://dx.doi.org/10.1016/j.saa.2014.11.007.

References

[1] M. Tümer, H. Köksal, M.K. Sener, S. Serin, Antimicrobial activity studies of the binuclear metal complexes derived from tridentate Schiff base ligands, Transition Met. Chem. 24 (1999) 414–420.
[2] S. Kumar, D.N. Dhar, P.N. Saxena, Applications of metal complexes of Schiff bases – a review, J. Sci. Ind. Res. 68 (2009) 181–187.
[3] S. Arulmurugan, H.P. Kavitha, B.R. Venkatraman, Biological activities of Schiff base and its complexes: a review, Rasayan J. Chem. 3 (2010) 385–410.
[4] U. Spichiger-Keller, Chemical Sesors and Biosensors for Medical and Biological Applications, Wiley-VCH, Weinheim, 1998.
[5] E. Jungreis, S. Thabet, Analytical Applications of Schiff bases, Marcell Dekker, New York, 1969.
[6] M.N. Ibrahim, S.E.A. Sharif, Synthesis, characterization and use of Schiff bases as fluorimetric analytical reagents, E-. J. Chem. 4 (2007) 531–535.
[7] C.M. da Silva, D.L. da Silva, L.V. Modolo, R.B. Alves, M.A. de Resende, C.V.B. Martins, A. de Fatima, Schiff bases: a short review of their antimicrobial activities, J. Adv. Res. 2 (2011) 1–8.
[8] A. Mohindru, J.M. Fisher, M. Rabinovitz, Bathocuproine sulphonate: a tissue culture-compatible indicator of copper-mediated toxicity, Nature (London) 303 (1983) 64.
[9] F. Basolo, B.M. Hoffman, J.A. Ibers, Synthetic oxygen carriers of biological interest, Acc. Chem. Res. 8 (1975) 384–392.
[10] A.C.W. Leung, M.J. MacLachlan, Schiff base complexes in macromolecules, J. Inorg. Organomet. Polym Mater. 17 (2007) 57–89.
[11] Y.P. Tian, C.Y. Duan, C.Y. Zhao, X.Z. You, T.C.W. Mak, Z. Zhang, Synthesis, crystal structure, and second-order optical nonlinearity of bis(2-chlorobenzaldehyde thiosemicarbazone)cadmium halides (CdL_2X_2; X = Br, I), Inorg. Chem. 36 (1997) 1247–1252.
[12] S. Karabocek, S. Guner, N.J. Karabocek, Models for copper-proteins: Structure and properties of dimeric copper(I) and (II) complexes of a tetraamino-tetrathioether ligand, J. Inorg. Biochem. 66 (1997) 57–61.
[13] R.E. Hester, E.M. Nour, Resonance Raman studies of transition metal peroxo complexes: 5—The oxygen carrier cobalt(II)-salen and its μ-peroxo complexes, $[(L)(salen)Co]_2O_2$; L = DMSO, py, DMF, pyO and no L†, J. Raman Spectrosc. 11 (1981) 49–58.
[14] T. Sedaghat, S. Menati, Synthesis and spectroscopic characterization of new adducts of diorganotin(IV) dichlorides with an asymmetric schiff base ligand, Inorg. Chem. Commun. 7 (2004) 760–762.
[15] E. Pereira, L.R. Gomes, J.N. Low, B. de Castro, Synthesis, spectroscopic, electrochemical and structural characterization of Cu(II) complexes with asymmetric NN′OS coordination spheres, Polyhedron 27 (2008) 335–343.
[16] A. Huber, L. Muller, H. Elias, R. Klement, M. Valko, Cobalt(II) complexes with substituted salen-type ligands and their dioxygen affinity in N, N-dimethylformamide at various temperatures, Eur. J. Inorg. Chem. 8 (2005) 1459–1467.
[17] E.J. Campbell, S.T. Nguyen, Unsymmetrical salen-type ligands: high yield synthesis of salen-type Schiff bases containing two different benzaldehyde moieties, Tetrahedron Lett. 42 (2001) 1221–1225.
[18] A.W. Kleij, Nonsymmetrical salen ligands and their complexes: synthesis and applications, Eur. J. Inorg. Chem. 2 (2009) 193–205.
[19] A.D. Cort, F. Gasparrini, L. Lunazzi, L. Mandolini, A. Mazzanti, C. Pasquini, M. Pierini, R. Rompietti, L. Schiaffino, Stereomutations of atropisomers of sterically hindered salophen ligands, J. Org. Chem. 70 (2005) 8877–8883.
[20] M.J. O'Donnell, The enantioselective synthesis of α-amino acids by phase-transfer catalysis with achiral Schiff base esters, Acc. Chem. Res. 37 (2004) 506–517.
[21] K.C. Gupta, A.K. Sutar, Catalytic activities of Schiff base transition metal complexes, Coord. Chem. Rev. 252 (2008) 1420–1450.
[22] L. Canali, D.C. Sherrington, Utilisation of homogeneous and supported chiral metal(salen) complexes in asymmetric catalysis, Chem. Soc. Rev. 28 (1999) 85–93.
[23] P.G. Cozzi, Metal-Salen Schiff base complexes in catalysis: practical aspects, Chem. Soc. Rev. 33 (2004) 410–421.
[24] F. Faridbod, M.R. Ganjali, R. Dinarvand, P. Norouzi, S. Riahi, Schiff's bases and crown ethers as supramolecular sensing materials in the construction of potentiometric membrane sensors, Sensors 8 (2008) 1645–1703.
[25] P.G. Lacroix, Second-order optical nonlinearities in coordination chemistry: the case of bis(salicylaldiminato)metal Schiff base complexes, Eur. J. Inorg. Chem. 2 (2001) 339–348.
[26] E. Hadjoudis, I.M. Mavridis, Photochromism and thermochromism of Schiff bases in the solid state: structural aspects, Chem. Soc. Rev. 33 (2004) 579–588.
[27] M. Andruh, Compartmental Schiff-base ligands—a rich library of tectons in designing magnetic and luminescent materials, Chem. Commun. 47 (2011) 3025–3042.
[28] H. Miyasaka, A. Saitoh, S. Abe, Magnetic assemblies based on Mn(III) salen analogues, Coord. Chem. Rev. 251 (2007) 2622–2664.
[29] A. Majumder, G.M. Rosair, A. Mallick, N. Chattopadhyay, S. Mitra, Synthesis, structures and fluorescence of nickel, zinc and cadmium complexes with the N, N, O-tridentate Schiff base N-2-pyridylmethylidene-2-hydroxy-phenylamine, Polyhedron 25 (2006) 1753–1762.
[30] C. Basu, S. Chowdhury, R. Banerjee, H. Stoeckli Evans, S. Mukherjee, A novel blue luminescent high-spin iron(III) complex with interlayer O—H···Cl bridging: synthesis, structure and spectroscopic studies, Polyhedron 26 (2007) 3617–3624.
[31] X.X. Zhou, H.C. Fang, Y.Y. Ge, Z.Y. Zhou, Z.G. Gu, X. Gong, G. Zhao, Q.G. Zhan, R.H. Zeng, Y.P. Cai, Assembly of a series of trinuclear Zinc(II) compounds with N_2O_2 donor tetradentate symmetrical Schiff base ligand, Cryst. Growth Des. 10 (2010) 4014–4022.
[32] S. Khatua, S.H. Choi, J. Lee, K. Kim, Y. Do, D.G. Churchill, Aqueous fluorometric and colorimetric sensing of phosphate ions by a fluorescent dinuclear Zinc complex, Inorg. Chem. 48 (2009) 2993–2999.
[33] T. Kawamoto, M. Nishiwaki, Y. Tsunekawa, K. Nozaki, T. Konno, Synthesis and characterization of luminescent Zinc(II) and Cadmium(II) complexes with N,S-chelating Schiff base ligands, Inorg. Chem. 47 (2008) 3095–3104.
[34] Y.S. Song, B. Yan, Z.X. Chen, Synthesis of two luminescent coordination polymers based on self-assembly of Zn(II) with polycarboxylic acids ligands and heteroaromatic N-donor, Appl. Organomet. Chem. 20 (2006) 44–50.
[35] S. Naskar, S. Naskar, H.M. Figgie, W.S. Sheldrick, S.K. Chattopadhyay, Synthesis, crystal structures and spectroscopic properties of two Zn(II) Schiff's base complexes of pyridoxal, Polyhedron 29 (2010) 493–499.
[36] S. Deshpande, D. Srinivas, P. Ratnasamy, EPR and catalytic investigation of Cu(Salen) complexes encapsulated in zeolites, J. Catal. 188 (1999) 261–269.
[37] M.F. Zaltariov, M. Cazacu, N. Vornicu, S. Shova, C. Racles, M. Balan, C. Turta, A new diamine containing disiloxane moiety and some derived Schiff bases: synthesis, structural characterisation and antimicrobial activity, Supramol. Chem. 25 (2013) 490–502.
[38] A. Soroceanu, M. Cazacu, S. Shova, C. Turta, J. Kozisek, M. Gall, M. Breza, P. Rapta, T.C.O. Mac Leod, A.J.L. Pombeiro, J. Telser, A.A. Dobrov, V.B. Arion, Copper(II) complexes with Schiff bases containing a disiloxane unit: synthesis, structure, bonding features and catalytic activity for aerobic oxidation of benzyl alcohol, Eur. J. Inorg. Chem. 9 (2013) 1458–1474.
[39] T. Yamamoto, K. Kojiri, H. Morishima, H. Naganawa, T. Aoyagi, H. Umezawa, The structure of forphenicine, J. Antibiot. 31 (1978) 483–484.
[40] A. Prakash, D. Adhikari, Application of Schiff bases and their metal complexes – a Review, Int. J. Chem. Tech. Res. 3 (2011) 1891–1896.
[41] CrysAlisRED, Oxford Diffraction Ltd., Version 1.171.34.76, 2003.

[42] O.V. Dolomanov, L.J. Bourhis, R.J. Gildea, J.A.K. Howard, H. Puschmann, OLEX2: a complete structure solution, refinement and analysis program, J. Appl. Cryst. 42 (2009) 339–341.
[43] G.M. Sheldrick, A short history of SHELX, Acta Cryst. A 64 (2008) 112–122.
[44] S. Mitra, N. Tamai, A combined experimental and theoretical study on the photochromism of aromatic anils, Chem. Phys. 246 (1999) 463–475.
[45] V. Vargas, L. Amigo, A study of the tautomers of N-salicylidene-p-X-aniline compounds in methanol, J. Chem. Soc. Perkin Trans. 2 (2001) 1124–1129.
[46] M. Ziolek, J. Kubicki, A. Maciejewski, R. Naskrcki, A. Grabowska, Enol-keto tautomerism of aromatic photochromic Schiff base N, N′-bis(salicylidene)-p-phenylenediamine: ground state equilibrium and excited state deactivation studied by solvatochromic measurements on ultrafast time scale, J. Chem. Phys. 124 (2006) 124518.
[47] K. Ogawa, J. Harada, T. Fujiwara, S. Yoshida, Thermochromism of salicylideneanilines in solution: aggregation-controlled proton tautomerization, J. Phys. Chem. A 105 (2001) 3425–3427.